

# Reactions of VX, GB, GD, and HD with Nanosize Al<sub>2</sub>O<sub>3</sub>. Formation of Aluminophosphonates

George W. Wagner,<sup>\*,†</sup> Lawrence R. Procell,<sup>†</sup> Richard J. O'Connor,<sup>†</sup> Shekar Munavalli,<sup>‡</sup> Corrie L. Carnes,<sup>§</sup> Pramesh N. Kapoor,<sup>§</sup> and Kenneth J. Klabunde<sup>§</sup>

Contribution from the Research and Technology Directorate, U.S. Army Edgewood Chemical Biological Center, Aberdeen Proving Ground, Maryland 21010, Geo-Centers, Inc., Gunpowder Branch Box 68, Aberdeen Proving Ground, Maryland 21010, and Department of Chemistry, Kansas State University, and Nantek, Inc., 1500 Hayes Dr., Manhattan, Kansas 66502

Received September 27, 2000

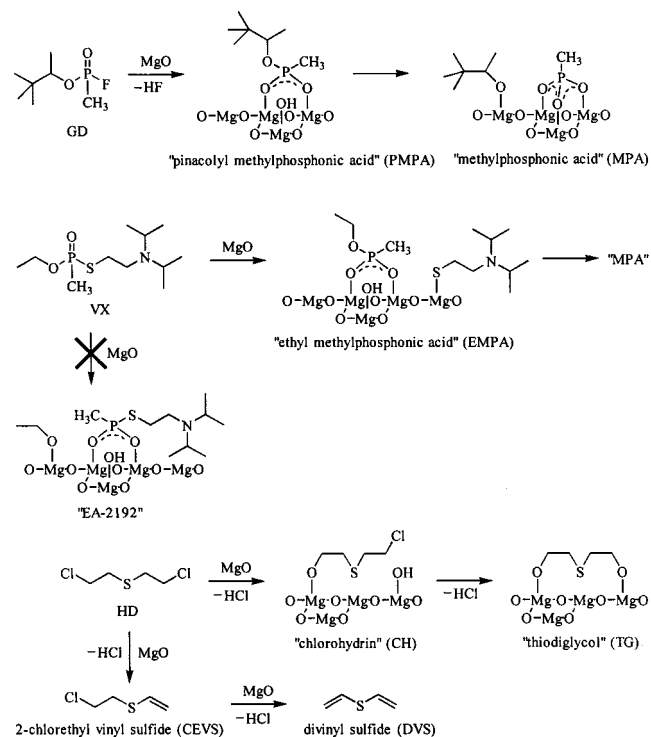
**Abstract:** Room-temperature reactions of VX, GB, GD, and HD with nanosize Al<sub>2</sub>O<sub>3</sub> (AP-Al<sub>2</sub>O<sub>3</sub>) have been characterized by <sup>31</sup>P, <sup>13</sup>C, and <sup>27</sup>Al MAS NMR. Nerve agents VX, GB, and GD hydrolyze to yield surface-bound complexes of their corresponding nontoxic phosphonates. At sufficiently high loadings, discreet aluminophosphonate complexes, Al[OP(O)(CH<sub>3</sub>)OR]<sub>3</sub>, are generated which are identical to synthesized model compounds. Thus the reaction with phosphonic acids is not just surface-limited, but can continue to the core of alumina particles. HD mainly hydrolyzes at lower loadings to yield thiodiglycol (TG, 71%) and a minor amount of the CH-TG sulfonium ion (12%), although some elimination of HCl is also observed (17%). The reactive capacity for HD is evidently exceeded at high loadings, where complete conversion to TG is hindered. However, addition of excess water results in the quantitative hydrolysis of sorbed HD to CH-TG. On AP-Al<sub>2</sub>O<sub>3</sub> dried to remove physisorbed water, <sup>13</sup>C CP-MAS NMR detects a surface alkoxide consistent with that of TG.

## Introduction

Inorganic oxides are currently being considered as reactive sorbents for the decontamination of chemical warfare agents (CWA).<sup>1</sup> These versatile materials, well-known for their industrial uses as adsorbents, catalysts, and catalyst supports, have many potential decontamination applications such as environmentally friendly "hasty" decontamination on the battlefield, protective filtration systems for vehicles, aircraft, and buildings, and the demilitarization of CWA munitions and stockpiles. To stress the enormity of the latter problem, the U.S. and Russia have declared CWA stockpiles of 25 000 and 42 000 tons, respectively.<sup>1b</sup>

Previous work has demonstrated room-temperature reactions of VX [O-ethyl S-(2-diisopropylamino)ethyl methylphosphonothioate], GD (pinacolyl methylphosphonofluoridate), and HD [bis(2-chloroethyl) sulfide] with nanosize MgO (AP-MgO)<sup>2</sup> and CaO (AP-CaO).<sup>3</sup> The nerve agents VX and GD hydrolyze on the metal oxides as shown for MgO in Scheme 1. These reactions are analogous to their solution behavior<sup>1a</sup> with two exceptions. The first is that the corresponding nontoxic phos-

## Scheme 1



\* Address correspondence of this author. Tel: (410) 436-8468. FAX: (410) 436-7317. E-mail: george.wagner@sbcom.apgea.army.mil.

<sup>†</sup> Research and Technology Directorate, U.S. Army Edgewood Chemical Biological Center.

<sup>‡</sup> Geo-Centers, Inc., Gunpowder Branch Box 68.

<sup>§</sup> Kansas State University and Nantek, Inc.

(1) (a) Yang, Y.-C.; Baker, J. A.; Ward, J. R. *Chem. Rev.* **1992**, *92*, 1729–1743. (b) Yang, Y.-C. *Acc. Chem. Res.* **1999**, *32*, 109–115 and references therein. (c) Yang, Y.-C.; Szafraniec, L. L.; Beaudry, W. T. *J. Org. Chem.* **1993**, *58*, 6964–6965. (d) Bartram, P. W.; Wagner, G. W. U.S. Patent No. 5,689,038, Nov. 18, 1997.

(2) Wagner, G. W.; Bartram, P. W.; Koper, O.; Klabunde, K. J. *J. Phys. Chem. B* **1999**, *103*, 3225–3228.

(3) Wagner, G. W.; Koper, O.; Lucas, E.; Decker, S.; Klabunde, K. J. *J. Phys. Chem. B* **2000**, *104*, 5118–5123.

phonate products reside as surface-bound complexes. The second and most notable exception is that toxic EA-2192, which forms under basic hydrolysis,<sup>1b,c</sup> is not observed on AP-MgO and AP-CaO, nor on other inorganic oxides examined,<sup>4</sup> including

(4) Wagner, G. W.; Bartram, P. W. Unpublished results.

zeolites.<sup>5</sup> Such selectivity for VX hydrolysis is shown in the slow reaction of VX with an equimolar amount of water.<sup>6</sup> Although hydrolysis is similarly observed for HD, elimination of HCl is also a major reaction pathway (Scheme 1). On AP-MgO<sup>2</sup> the product distribution was 50% thiodiglycol (TG) and 50% divinyl sulfide (DVS). However, HD on AP-CaO<sup>3</sup> exhibited autocatalytic dehydrohalogenation behavior where up to 80% DVS formed along with TG and minor amounts of the sulfonium ion CH-TG (Scheme 1). The kinetics and product stream were quite sensitive to the hydration state of the AP-CaO,<sup>3</sup> which was attributed to acid-catalyzed surface reconstruction and formation of CaCl<sub>2</sub>, which is known to be a more active dehydrohalogenation catalyst than CaO.<sup>7</sup> The broadened nature of the <sup>13</sup>C MAS NMR peaks observed for TG on AP-MgO and AP-CaO suggested that this product resides as a surface-bound alkoxide.

Using IR, Kuiper et al.<sup>8</sup> and Yates et al.<sup>9</sup> have detected alumina surface-bound isopropyl methylphosphonate (the hydrolysis product of GB) and 2-hydroxyethyl ethyl sulfide (the hydrolysis product of 2-chloroethyl ethyl sulfide, CEES, a common HD simulant), respectively. MAS NMR has also provided evidence for these species on AP-MgO<sup>2</sup> and AP-CaO.<sup>3</sup> For VX and GD, broadened <sup>31</sup>P MAS NMR peaks, indicative of restricted mobility, were detected for the phosphonate products. Moreover, spinning sidebands consistent with the expected large chemical shift anisotropy (CSA)<sup>10</sup> of these species, which is not averaged by motion,<sup>11</sup> were also evident. For HD, broadened <sup>13</sup>C MAS NMR peaks were also found for the TG product, again indicative of surface immobilization. In the present study, <sup>27</sup>Al, in addition to <sup>31</sup>P and <sup>13</sup>C, MAS NMR is employed to better characterize the surface complexes of these products on nanosize Al<sub>2</sub>O<sub>3</sub> (AP-Al<sub>2</sub>O<sub>3</sub>). Spectra of the surface-bound phosphonate products are compared to those of synthesized aluminophosphate model compounds, which were prepared by simple precipitation reactions.<sup>12</sup> Hypothetical structures for these latter compounds are shown in Figure 1 (see Discussion).

<sup>27</sup>Al MAS NMR is also employed to characterize structural details of the AP-Al<sub>2</sub>O<sub>3</sub>, which provides information on the distribution of tetrahedrally (*T<sub>d</sub>*) and octahedrally (*O<sub>h</sub>*) coordinated aluminum atoms. Additionally, <sup>27</sup>Al Cross-Polarization (CP) MAS NMR is used to characterize the coordination of surface aluminum atoms.<sup>13</sup> Surface aluminum atoms are associated with hydroxyls existing on the surfaces of  $\gamma$ - and  $\eta$ -aluminas, and higher surface area aluminas.<sup>14,15</sup> Knozinger and Ratnasamy<sup>15</sup> have proposed structures for five types which are also given in Figure 1.

Knozinger and Ratnasamy<sup>15</sup> assigned five hydroxyl IR bands detected on  $\gamma$ - and  $\eta$ -aluminas to the five hydroxyl structures based on their net charge, with type Ia being the most basic and type III being the most acidic. The most basic hydroxyls

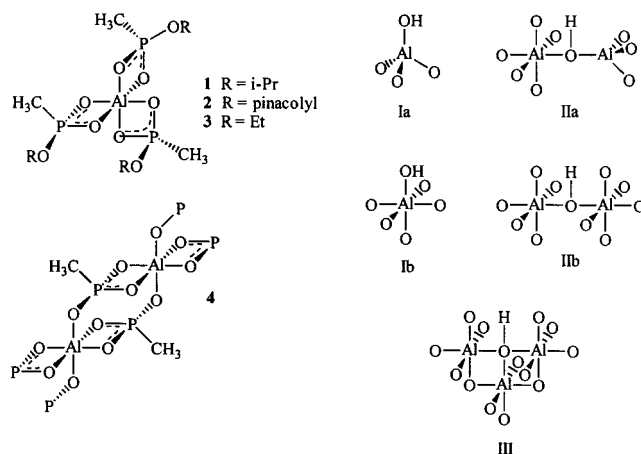
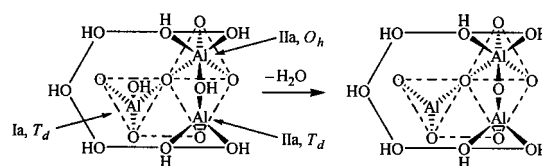


**Figure 1.** Hypothetical structures of compounds 1–4 and structures of five hydroxyl groups proposed to exist on high surface area aluminas.

### Scheme 2



are removed first during dehydroxylation, and these are the hydroxyls bound to *T<sub>d</sub>* aluminum atoms, i.e., Ia and IIa. Consistent with their ease of dehydroxylation, Ia and Ib undergo facile oxygen exchange with C<sup>18</sup>O<sub>2</sub> at room temperature, while the oxygens of the other hydroxyl sites exchange much more slowly.<sup>16,17</sup> Additionally, Knozinger and Ratnasamy<sup>15</sup> noted that type Ia hydroxyls may rotate around their single Al–O bond, thus facilitating H-bonding with neighboring groups and, perhaps, dehydroxylation. The type IIa hydroxyls, however, are anchored by two bonds and are not free to rotate. Dehydroxylation at low temperatures (<770 K) occurs via removal of adjacent hydroxyls and does not require OH migration. A particularly favorable dehydroxylation is envisioned for the nearest neighbor Ia and IIa sites on the (111) face of alumina. This mechanism is shown in Scheme 2. Nearest neighbors (in plane) in the bottom oxide layer are connected by dashed lines and nearest neighbors (in plane) in the top hydroxide layer are connected by solid lines (some have been omitted for clarity). The aluminum atoms are sandwiched in the middle layer, and their coordination with the top and bottom layers is as indicated. Removal of OH from the more basic Ia site and deprotonation of the more acidic IIa site to evolve water generates a coordinatively unsaturated, 3-coordinate Al<sup>3+</sup> Lewis acid site (in a *T<sub>d</sub>* site) and a coordinatively unsaturated oxygen Lewis base site bridging *T<sub>d</sub>* and *O<sub>h</sub>* aluminum sites. At higher temperatures (above 940 K) extreme dehydroxylation involves aluminum and oxide migration, with concomitant generation of the high-temperature phase  $\alpha$ -alumina possessing only *O<sub>h</sub>* aluminum sites. Quite recently, Sohlberg et al.<sup>18</sup> proposed that surface 3-coordinate Al<sup>3+</sup> sites are not stable, and can relax into vacant octahedral sites to become six-coordinate, thus offering an explanation as to why 3-coordinate Al<sup>3+</sup> sites have not been observed by <sup>27</sup>Al NMR<sup>19</sup> (see below). In view of such potential

(5) Wagner, G. W.; Bartram, P. W. *Langmuir* **1999**, *15*, 8113–8118.  
 (6) Yang, Y.-C.; Szafraniec, L. L.; Beaudry, W. T.; Rohrbaugh, D. K.; Procell, L. R.; Samuel, J. B. *J. Org. Chem.* **1996**, *61*, 8407–8413.  
 (7) Noller, H.; Hantsche, H.; Andreu, P. *J. Catal.* **1965**, *4*, 354–362.  
 (8) Kuiper, A. E. T.; van Bokhoven, J. J. G. M.; Medema, J. *J. Catal.* **1976**, *43*, 154–167.  
 (9) Mawhinney, D. B.; Rossin, J. A.; Gerhart, K.; Yates, J. T., Jr. *Langmuir* **1999**, *15*, 4789–4795.  
 (10) Duncan, T. M.; Douglass, D. C. *Chem. Phys.* **1984**, *87*, 339–349.  
 (11) (a) Vila, A. J.; Lagier, C. M.; Wagner, G.; Olivieri, A. C. *J. Chem. Soc., Chem. Commun.* **1991**, 683–685. (b) Olivieri, A. C. *J. Magn. Reson.* **1990**, *88*, 1–8.  
 (12) Cao, G.; Lee, H.; Lynch, V. M.; Mallouk, T. E. *Inorg. Chem.* **1988**, *27*, 2781–2785.  
 (13) Morris, H. D.; Ellis, P. D. *J. Am. Chem. Soc.* **1989**, *111*, 6045–6049.  
 (14) Peri, J. B.; Hannan, R. B. *J. Phys. Chem.* **1960**, *64*, 1526.  
 (15) Knozinger, H.; Ratnasamy, P. *Catal. Rev. Sci. Eng.* **1978**, *17*, 31.

(16) Peri, J. B. *J. Phys. Chem.* **1975**, *79*, 1582.  
 (17) Amenomiya, A.; Morikawa, Y.; Pleizier, G. *J. Catal.* **1977**, *46*, 431.  
 (18) Sohlberg, K.; Pennycook, S. J.; Pantelides, S. T. *J. Am. Chem. Soc.* **1999**, *121*, 10999–11001.  
 (19) Coster, D.; Blumenfeld, A. L.; Fripiat, J. J. *J. Phys. Chem.* **1994**, *98*, 6201–6211.

surface reconstruction, the 3-coordinate  $\text{Al}^{3+}$  site in Scheme 2 should perhaps be considered a transient intermediate species.

Such dramatic changes in the coordination of aluminum sites following hydroxylation/dehydroxylation (and, as we shall see, their reactions with chemical warfare agents) have profound implications for their detection by  $^{27}\text{Al}$  MAS NMR. This is due to the fact that low symmetry sites possess large electric field gradients, resulting in large quadrupolar coupling constants ( $Q_{cc}$ ) and extreme NMR line broadening. This problem is lessened at higher magnetic fields as  $Q_{cc}$  remains constant, and the NMR Zeeman interaction begins to dominate the line shape. Historically, "hidden" aluminum in aluminum oxide has been of concern owing to suspected large  $Q_{cc}$ 's for aluminum sites near the surface.<sup>20</sup> Huggins and Ellis<sup>21</sup> have calculated the  $Q_{cc}$ 's for the various aluminum sites near the surface of  $\gamma$ -alumina. All of the hydroxyl sites mentioned above possessed reasonable  $Q_{cc}$ 's (<12 MHz) which would not prevent their detection. However,  $Q_{cc}$ 's for coordinatively unsaturated, pentacoordinate  $\text{Al}^{3+}$  Lewis acid sites were quite large (ca. 25 MHz).  $Q_{cc}$ 's for 3-coordinate sites were not calculated, and these sites have not been observed by  $^{27}\text{Al}$  NMR.<sup>19</sup> Indeed, their very existence is questioned.<sup>18,19</sup> Employing static (i.e. no MAS)  $^{27}\text{Al}$  NMR at a field of 9.4 T, Huggins and Ellis<sup>21</sup> detected resonances for only the  $T_d$  and  $O_h$  sites, and found that not all of the aluminum in  $\gamma$ -alumina was observable at room temperature. However, some of the "invisible" aluminum was recovered at low temperature. This observation led Huggins and Ellis<sup>21</sup> to propose a dynamic mechanism for the obscuration of surface aluminum based on water exchange and motion. Such motion could facilitate quadrupolar relaxation resulting in broadened lines. Recently, Maciel et al.<sup>22</sup> obtained  $^{27}\text{Al}$  MAS NMR spectra of  $\gamma$ -alumina at 14 T, and detected pentacoordinated aluminum sites in addition to the  $T_d$  and  $O_h$  sites. Regarding the question of "invisible" aluminum sites, Maciel et al.<sup>22</sup> found that all of the aluminum is observed at 14 T. In the current work, a high surface area  $\gamma$ -alumina is examined at 7 T by  $^{27}\text{Al}$  MAS NMR at various stages of dehydroxylation and at low temperature to further probe the nature of "invisible" aluminum sites.

## Experimental Section

**Materials.** Nanosize  $\text{Al}_2\text{O}_3$  (AP- $\text{Al}_2\text{O}_3$ ) was synthesized from an aluminum ethoxide precursor. The material was activated by heating under a dynamic vacuum, pausing 1 h at every 50 °C interval to 500 °C, and kept at that temperature overnight. The resulting material was light-gray in appearance and possessed a surface area of 273.6 m<sup>2</sup>/g. The  $\gamma$ -alumina used is Selexsorb CDX (Alcoa), and has a surface area of 400 m<sup>2</sup>/g. The aluminas were used as received, dried in air at 100 °C to remove physisorbed water, and dried in air at 400 °C to yield partially dehydroxylated aluminas (PDA). The AP- $\text{Al}_2\text{O}_3$  became white after the 400 °C treatment, which apparently burned-off residual carbonaceous material.  $^{13}\text{C}$ -labeled HD was used for the low-loading reaction with AP- $\text{Al}_2\text{O}_3$ .

**Aluminophosphonate Syntheses.** Aluminophosphonate model compounds were synthesized by mixing appropriate molar ratios of phosphonic acid and  $\text{Al}(\text{NO}_3)_3 \cdot 9\text{H}_2\text{O}$  (all from Aldrich) in water.  $\text{Al}[\text{OP}(\text{O})(\text{CH}_3)(\text{O}i\text{Pr})]_3$  (**1**) and  $\text{Al}[\text{OP}(\text{O})(\text{CH}_3)(\text{OPinacolyl})]_3$  (**2**) spontaneously precipitated and were filtered and dried under vacuum at room temperature to yield dry, white powders.  $\text{Al}[\text{OP}(\text{O})(\text{CH}_3)(\text{OEt})]_3$  (**3**) remained soluble, and attempts to precipitate it by raising the pH (NaOH) resulted in the predominant precipitation of aluminum hydroxide. Thus this compound, which is extremely hygroscopic, was isolated by drying under vacuum at 80 °C to yield a dry, white powder.

(20) O'Reilly, D. E. *Adv. Catal.* **1960**, *12*, 31.

(21) Huggins, B. A.; Ellis, P. D. *J. Am. Chem. Soc.* **1992**, *114*, 2098–2108.

(22) Fitzgerald, J. J.; Piedra, G.; Dec, S. F.; Seger, M.; Maciel, G. E. *J. Am. Chem. Soc.* **1997**, *119*, 7832–7842.

$\text{Al}_2[\text{OP}(\text{O})(\text{CH}_3)(\text{O})]_3$  (**4**), which also did not spontaneously precipitate, was isolated by adjusting the pH to 3 with NaOH to effect precipitation, followed by drying in air at 70 °C to yield a dry, white powder. Compounds **1**, **2**, and **4** are not hygroscopic. The compounds were analyzed by  $^{31}\text{P}$  and  $^{27}\text{Al}$  MAS NMR, which showed minor impurities of IMPA, PMPA, and MPA in **1**, **2**, and **4**, respectively. Analysis of **3** revealed possibly two crystal modifications for this compound (see Discussion).

**NMR.**  $^{31}\text{P}$ ,  $^{13}\text{C}$ , and  $^{27}\text{Al}$  MAS NMR spectra were obtained at 7 T with a Varian Unityplus 300 NMR spectrometer equipped with a Doty Scientific 7 mm high-speed VT-MAS probe. Additional  $^{27}\text{Al}$  MAS NMR spectra were obtained at 9.4 T with a Varian Inova 400 NMR spectrometer equipped with a Doty Scientific 7 mm super-sonic VT-MAS probe. Double O-ring sealed rotors (Doty Scientific) were used. Both direct polarization (DP) and cross-polarization (CP) spectra were obtained. For  $^{27}\text{Al}$  spectra, the 90° pulse width was determined by using 0.1 M  $\text{Al}(\text{NO}_3)_3 \cdot 9\text{H}_2\text{O}$ , which also served as the external shift reference. Quantitative spectra were obtained by using 0.2  $\mu\text{s}$  (3°) pulses.<sup>21</sup> For  $^{13}\text{C}$  and  $^{31}\text{P}$ , external TMS and 85%  $\text{H}_3\text{PO}_4$  were used as shift references.

**Reaction Procedure. Caution:** These experiments should only be performed by trained personnel using applicable safety procedures. In a typical kinetic run, 5 wt % neat, liquid agent (3–4  $\mu\text{L}$ ) was added via syringe to the center of a column of AP- $\text{Al}_2\text{O}_3$  (ca. 80 mg) contained in the NMR rotor. The rotor was then sealed with the double O-ring cap. MAS NMR spectra were obtained periodically to monitor the reaction in situ. Heavily loaded samples were prepared by adding 250  $\mu\text{mol}$  neat, liquid agent (30–70  $\mu\text{L}$ ) to 100 mg of AP- $\text{Al}_2\text{O}_3$  contained in a glass vial. The vial was capped and allowed to stand at room temperature for an extended period.

## Results and Discussion

**$^{27}\text{Al}$  MAS NMR Characterization of Aluminas.** To probe the effect of dehydroxylation on the creation of "invisible" aluminum sites, the aluminas were partially dehydroxylated (PD) at 400 °C and allowed to rehydroxylate by exposure to ambient air. Spectra for AP- $\text{Al}_2\text{O}_3$  and  $\gamma$ -alumina obtained at various stages of hydroxylation are shown in Figure 2. The broad peak at –70 ppm in the spectra is due to the probe background. Spectra of the fully hydrated materials on the right side of Figure 2 are identical with those of the "as received" material. The fully hydrated spectrum (Figure 2d) of the  $\gamma$ -alumina is typical,<sup>13,21,22</sup> showing both  $T_d$  and  $O_h$  sites at about 59.8 and 4.6 ppm, respectively. The fully hydrated AP- $\text{Al}_2\text{O}_3$  spectrum (Figure 2h) also reveals the presence of these sites, but the number of  $T_d$  sites is greatly reduced relative to the number of  $O_h$  sites. Also, compared to  $\gamma$ -alumina, the AP- $\text{Al}_2\text{O}_3$  resonance for the  $T_d$  sites is shifted to 71.2 ppm and broadened, while the shift (6.8 ppm) and broadness of the resonance for the  $O_h$  sites is comparable.

Significant changes in the spectra occur at various stages of dehydroxylation. The spectrum of PD  $\gamma$ -alumina reveals an extreme loss of intensity for the  $T_d$  sites relative to the  $O_h$  sites. Additionally, resonances for two  $T_d$  sites are resolved: a rather sharp peak at 58.5 ppm and a broader one at about 68.0 ppm. The spectrum of PD  $\gamma$ -alumina obtained at 9.4 T (Figure 2a) clearly resolves the resonances at 70.8 and 57.7 ppm, and exemplifies the greater resolution expected for quadrupolar nuclei at higher field. Based on the Knozinger–Ratnasamy model<sup>15</sup> for the various surface hydroxyl groups, and their propensity for dehydroxylation (i.e., Scheme 2), it is tempting to assign the sharp  $T_d$  resonance at 58.5 ppm to the Ia site, and the broader resonance at 68.0 ppm to the IIa site. Although this is precisely the behavior predicted by this model for mild dehydroxylation, more contemporary models suggest more complicated surface hydration interactions.<sup>23</sup> Thus additional

(23) Tsyganenko, A. A.; Mardilovich, P. P. *J. Chem. Soc., Faraday Trans.* **1996**, *92*, 4843–4852.

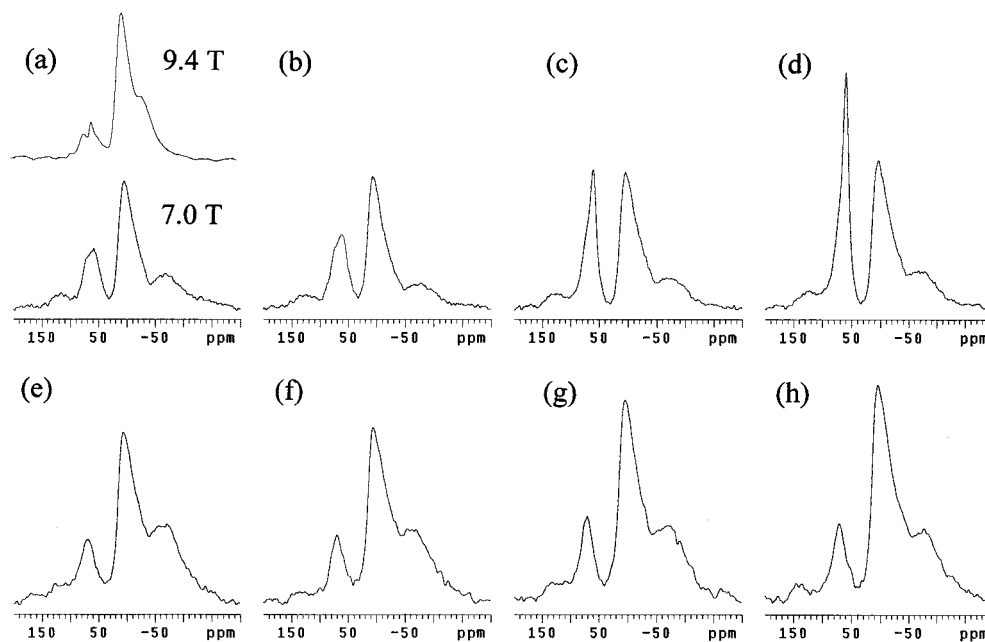


**Figure 2.**  $^{27}\text{Al}$  MAS NMR spectra of rehydroxylation of (a) PD  $\gamma$ -alumina (9.4 and 7.0 T, top series) and (e) PD AP- $\text{Al}_2\text{O}_3$  (7.0 T, bottom series). Weight gains are as follows: (b) 1.9%, (c) 6.2%, (d) 11.3%, (f) 2.0%, (g) 9.5%, and (h) 12.9%.

work is needed to understand the true nature of these hydration-dependent sites and their assignments to Ia and IIa must be considered tentative. For PD AP- $\text{Al}_2\text{O}_3$ , moderate loss in the  $O_h$  resonance intensity relative to the  $T_d$  resonance is observed. This behavior indicates a fundamental difference in the surfaces of these aluminas, i.e., AP- $\text{Al}_2\text{O}_3$  does not possess the  $T_d$  type Ia sites found in  $\gamma$ -alumina. Rather, primary dehydroxylation of AP- $\text{Al}_2\text{O}_3$  occurs predominately at  $O_h$  sites, presumably type Ib. The fact that less intensity loss is observed for PD AP- $\text{Al}_2\text{O}_3$  compared to PD  $\gamma$ -alumina is consistent with the lower surface area of the PD AP- $\text{Al}_2\text{O}_3$  (273.6 vs 400  $\text{m}^2/\text{g}$ ), i.e., there is less surface relative to the bulk to dehydroxylate (and less corresponding signal loss).

Rehydroxylation of the  $\gamma$ -alumina causes recovery of the intensity of the sharp, Ia  $T_d$  site, along with a minor increase in intensity of the  $O_h$  sites. No noticeable increase in intensity is observed for the broader, IIa  $T_d$  site. These observations are consistent with Scheme 2, where dehydroxylated site Ia loses its  $T_d$  symmetry to become a coordinatively unsaturated, 3-coordinate site. The  $Q_{cc}$  for a site of this geometry was not calculated by Huggins and Ellis,<sup>21</sup> but either it is evidently large enough to prevent its detection at 7 T or, alternatively, the site undergoes surface rearrangement to increase its coordination.<sup>18</sup> Even at 14 T, Maciel et al.<sup>22</sup> did not detect 3-coordinate sites in PD alumina, perhaps consistent with surface rearrangement of the site. Regarding the other aluminum sites in Scheme 2, i.e., the  $O_h$  and  $T_d$  aluminum centers comprising the IIa site, dehydroxylation does not disturb their coordination number; thus they remain detectable in either the hydroxylated or dehydroxylated state. For PD AP- $\text{Al}_2\text{O}_3$ , rehydroxylation restores intensity primarily in the  $O_h$  sites. This can be envisioned to involve sites of the Ib type, where a coordinatively unsaturated, 5-coordinate aluminum is hydroxylated to restore its  $O_h$  symmetry. The five-coordinate site is evidently unobservable at 7 T, although Maciel et al.<sup>22</sup> did detect a 5-coordinate aluminum site at ca. 37 ppm at 14 T. For the rehydroxylation of PD AP- $\text{Al}_2\text{O}_3$  and  $\gamma$ -alumina, plots of weight gain vs gain in  $^{27}\text{Al}$  MAS peak area show similar behavior. Initial slopes for the two processes, e.g. rehydroxylation of the Ib  $O_h$  sites of PD AP- $\text{Al}_2\text{O}_3$  and the Ia sites of  $\gamma$ -alumina, are nearly identical, which is consistent with the idea

of titrating the coordinatively unsaturated aluminum sites with water to restore their NMR signals. The effect of this titration on signal intensity is also evidenced in  $^{27}\text{Al}$  CP-MAS NMR spectra (which selectively observes surface aluminum sites<sup>13</sup>) obtained for the same PD and fully hydroxylated samples as shown in Figure 3. For PD  $\gamma$ -alumina, low signal intensity is observed for the surface  $T_d$  and  $O_h$  sites, but the intensity increases for the fully hydroxylated  $\gamma$ -alumina. For AP- $\text{Al}_2\text{O}_3$ , the CP spectra reflect the increase in intensity of the  $O_h$  site (rather than the  $T_d$  site) as the surface is hydroxylated.

A spectrum was acquired for PD  $\gamma$ -alumina at  $-100$  °C to assess the extent to which the signal loss at the tentatively assigned Ia  $T_d$  site may be due to a dynamic process. Spectra were also acquired immediately before and after subjecting the sample to  $-100$  °C. Owing to Boltzmann enhancement at low temperature,<sup>21</sup> the  $O_h$  peaks of the room-temperature spectra were normalized to the greater intensity of the  $O_h$  peak in the  $-100$  °C spectrum to facilitate observing intensity changes at the  $T_d$  sites. In the  $-100$  °C spectrum, there is a small, but observable increase in the intensity of the Ia  $T_d$  site peak relative to those of the IIa  $T_d$  and  $O_h$  sites, and the original intensity is restored upon return to room temperature. These observations are consistent with a small contribution to the obscuration of the Ia site due to surface OH exchange dynamics in agreement with the mechanism proposed by Huggins and Ellis.<sup>21</sup> However, such exchange is not the major cause of the "invisible", tentatively assigned dehydroxylated Ia  $T_d$  sites, and other causes such as extensive surface reconstruction<sup>18</sup> or possibly an enormous  $Q_{cc}$  for these coordinatively unsaturated 3-coordinate sites<sup>19</sup> must be considered.

**Low-Loading Agent Reactions with AP- $\text{Al}_2\text{O}_3$ .** Selected  $^{31}\text{P}$  and  $^{13}\text{C}$  MAS NMR spectra obtained for the reactions of 5 wt % VX, GD, and HD ( $^{13}\text{C}$  labeled) with "as received" AP- $\text{Al}_2\text{O}_3$  are shown in Figure 4. NMR shifts and assignments are given in Table 1. The reaction profiles are shown in Figure 5. The reaction observed for VX (sharp peak at 52.0 ppm) is consistent with Scheme 1, where the hydrolysis is selective for ethyl methylphosphic acid (EMPA, broad peak at 23 ppm). No toxic

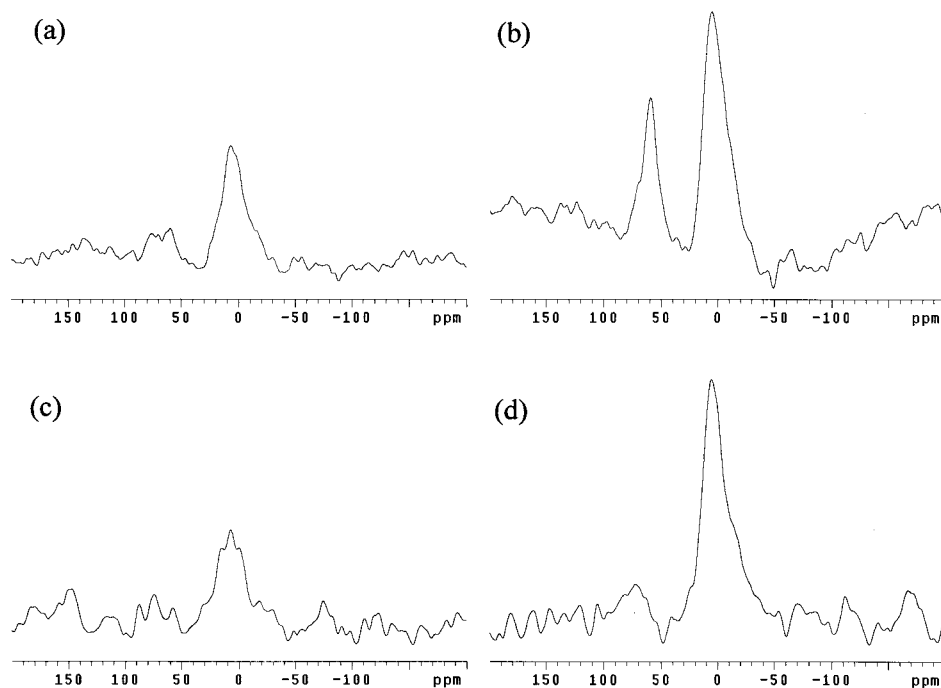


**Figure 3.**  $^{27}\text{Al}$  CP-MAS NMR spectra obtained for samples of Figure 2: (a) PD  $\gamma$ -alumina, (b) PD  $\gamma$ -alumina + 11.3 wt % water, (c) PD AP- $\text{Al}_2\text{O}_3$ , and (d) PD AP- $\text{Al}_2\text{O}_3$  + 12.9 wt % water.

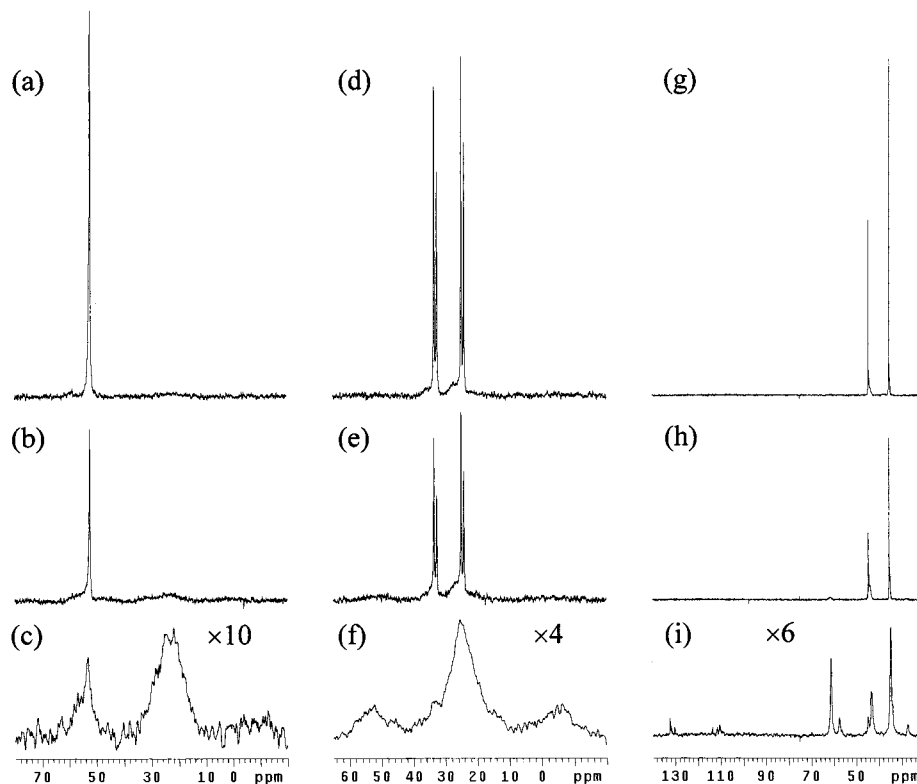


**Figure 4.** Selected MAS NMR spectra obtained for the reactions of 5 wt % VX ( $^{31}\text{P}$ , left), GD ( $^{31}\text{P}$ , middle), and HD ( $^{13}\text{C}$ , right) with “as received” AP- $\text{Al}_2\text{O}_3$ : (a) 11.5 min, (b) 24 h, (c) 15 days ( $\times 10$ ), (d) 9.5 min, (e) 1.0 h, (f) 8.0 h ( $\times 4$ ), (g) 11.5 min, (h) 1.0 h, and (i) 24 h ( $\times 6$ ).

EA-2192 is observed, which would yield a peak near 40 ppm.<sup>24</sup> This selectivity for EMPA has been previously observed on AP- $\text{MgO}^2$  and AP- $\text{CaO}$ .<sup>3</sup> The reaction observed for GD (sharp doublets centered near 29 ppm) is also identical with that in Scheme 1, affording pinacolyl methylphosphonic acid (PMPA, broad peak at 24 ppm). Finally, analogous to Scheme 1, HD

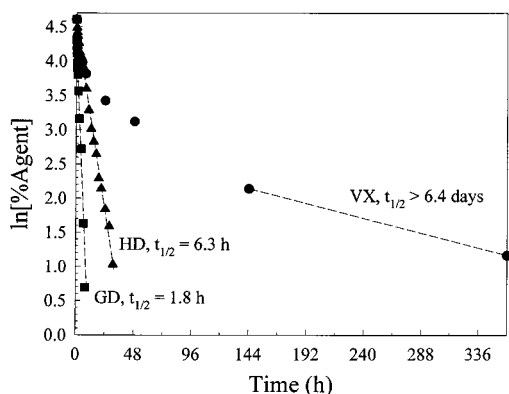
(sharp peaks at 44.6 and 35.4 ppm) primarily hydrolyzes to thiodiglycol (TG), with minor formation of the CH-TG sulfonium ion, 2-chloroethyl vinyl sulfide (CEVS), and divinyl sulfide (DVS). The ratio of hydrolysis to elimination is 83:17. Inspection of the reaction profiles in Figure 5 shows that the GD and HD reactions are characterized by fast, initial reactions followed by slower, diffusion-limited reactions exhibiting first-order behavior with half-lives of 1.8 and 6.3 h, respectively.

(24) Yang, Y.-C.; Szafraniec, L. L.; Beaudry, W. T.; Rohrbaugh, D. K. *J. Am. Chem. Soc.* **1990**, *112*, 6621.

**Table 1.** NMR Data for AP-Al<sub>2</sub>O<sub>3</sub>, Agents, Products, and Model Compounds

	species	nucleus/chemical shifts
AP-Al <sub>2</sub> O <sub>3</sub>	Al sites	<sup>27</sup> Al: 71.2 ( <i>T<sub>d</sub></i> ), 6.8 ( <i>O<sub>h</sub></i> )
AP-Al <sub>2</sub> O <sub>3</sub> + 6 M HCl	Al(H <sub>2</sub> O) <sub>6</sub> <sup>3+</sup>	<sup>27</sup> Al: 0.2
HD/AP-Al <sub>2</sub> O <sub>3</sub>	HD	<sup>13</sup> C: 44.6, 35.4
	TG	<sup>13</sup> C: 61.2, 34.5
	H-bonded TG	<sup>13</sup> C: 62.1, ca. 35 <sup>a</sup>
	TG-alkoxide	<sup>13</sup> C: ca. 75 <sup>a</sup> , ca. 35 <sup>a</sup>
	CH-TG	<sup>13</sup> C: 62.1, 57.6, 44.6, 34.5, 27.2
	H-2TG	<sup>13</sup> C: 57.6, 44.7, 42.2, 27.4
	CEVS	<sup>13</sup> C: 132.1, 110.3, 42.9, 33.7
	DVS	<sup>13</sup> C: 130.3, 113.4
	Al(H <sub>2</sub> O) <sub>6</sub> <sup>3+</sup>	<sup>27</sup> Al: 1.3
GB/AP-Al <sub>2</sub> O <sub>3</sub>	surface IMPA	<sup>31</sup> P: 22.5; <sup>13</sup> C: 67.8, 24.5, 13.4; <sup>27</sup> Al: not resolved
	<b>1</b>	<sup>31</sup> P: 14.4; <sup>13</sup> C: 67.8, 24.5, 13.4; <sup>27</sup> Al: -17.9
authentic <b>1</b>		<sup>31</sup> P: 12.6; <sup>13</sup> C: 68.5, 25.6, 14.9; <sup>27</sup> Al: -17.6
GD/AP-Al <sub>2</sub> O <sub>3</sub>	GD	<sup>31</sup> P: 29.3 ( <i>J<sub>PF</sub></i> = 1040), 28.4 ( <i>J<sub>PF</sub></i> = 1040)
	surface PMPA	<sup>31</sup> P: 23.4; <sup>13</sup> C: 79.5, 35.3, 26.2, 17.1, 13.1; <sup>27</sup> Al: not resolved
	<b>2</b>	<sup>31</sup> P: 14.3; <sup>13</sup> C: 79.5, 35.3, 26.2, 17.1, 13.1; <sup>27</sup> Al: -12.2
authentic <b>2</b>		<sup>31</sup> P: 14.3; <sup>13</sup> C: 80.0, 36.7, 27.8, 18.8, 15.3; <sup>27</sup> Al: -16.7
VX/AP-Al <sub>2</sub> O <sub>3</sub>	VX	<sup>31</sup> P: 52.0
	surface EMPA	<sup>31</sup> P: 23.0
	MPA <sup>b</sup>	<sup>31</sup> P: 17.3; <sup>13</sup> C: 12.6; <sup>a</sup> <sup>27</sup> Al: not resolved
	hydrated <b>3</b>	<sup>31</sup> P: 21.0; <sup>13</sup> C: 59.8, 17.1, 12.6; <sup>27</sup> Al: -15.5
authentic <b>3</b>	phase 1 <sup>c</sup>	<sup>31</sup> P: 19.7; <sup>13</sup> C: 59.2, 17.5, 16.1, 14.5 ( <i>J<sub>PF</sub></i> = 130); 13.3 ( <i>J<sub>PF</sub></i> = 130); <sup>27</sup> Al: -14.9
	phase 2 <sup>d</sup>	<sup>31</sup> P: 18.0; <sup>13</sup> C: 59.2, 17.5, 16.1, 14.5 ( <i>J<sub>PF</sub></i> = 130); 13.3 ( <i>J<sub>PF</sub></i> = 130); <sup>27</sup> Al: -14.9
authentic <b>4</b>		<sup>31</sup> P: 18.6; <sup>13</sup> C: 14.4 ( <i>J<sub>PF</sub></i> = 133); <sup>27</sup> Al: -14.6

<sup>a</sup> Overlaps the larger peak in the spectrum. <sup>b</sup> Either surface bound or **4**. <sup>c</sup> Tentatively assigned to the hydrated phase. <sup>d</sup> Tentatively assigned to the anhydrous phase.

**Figure 5.** Reaction profiles for the reactions of 5 wt % VX, GD, and HD with “as received” AP-Al<sub>2</sub>O<sub>3</sub>.

VX also exhibits a rather fast, initial reaction, but the diffusion-limited reaction is much slower with a half-life greater than 6.4 days. The fast reactions are attributed to facile liquid spreading through the pores across fresh, unreacted surface. Spreading stops once the liquid achieves its volume in the pores; the reaction ceases, too, once the surface is consumed with product. The mechanism by which fresh surface is reached is via evaporation and gas-phase diffusion. Consistent with this latter mechanism, the diffusion-limited half-lives observed for GD, HD, and VX are in relative agreement with their vapor pressures: 0.4, 0.072, and 0.0007 mmHg, respectively.

**High-Loading Agent Reactions with AP-Al<sub>2</sub>O<sub>3</sub>.** In previous work with AP-MgO<sup>2</sup> and AP-CaO,<sup>3</sup> surface complexes were formed by the phosphonic acid products of VX and GD, and it was proposed that the HD product TG resided as a surface alkoxide (Scheme 1). High loadings of GB (Sarin, isopropyl methylphosphonofluoridate), GD, VX, and HD were employed to facilitate the use of <sup>27</sup>Al MAS NMR to characterize the potential surface complexes of these products on AP-Al<sub>2</sub>O<sub>3</sub>. For each sample a 250 μmol agent was reacted with 100 mg of AP-Al<sub>2</sub>O<sub>3</sub>, nominally 980 μmol (ignoring water weight); thus

the molar loading was kept constant. Model compounds of the phosphonic acid surface complexes, i.e., aluminophosphonates Al[OP(O)(CH<sub>3</sub>)(OR)]<sub>3</sub> [R = *i*-Pr (**1**), pinacolyl (**2**), and Et (**3**)] and Al<sub>2</sub>[OP(O)(CH<sub>3</sub>)(O)]<sub>3</sub> (**4**), were also prepared and characterized by MAS NMR to compare with the surface complexes.

<sup>13</sup>C and <sup>27</sup>Al MAS and <sup>27</sup>Al CP-MAS spectra obtained for 28 wt % HD (unlabeled) reacted with “as received” AP-Al<sub>2</sub>O<sub>3</sub> are shown in Figure 6. Such a loading apparently overwhelmed the reactive capacity of the AP-Al<sub>2</sub>O<sub>3</sub>. The <sup>13</sup>C MAS NMR spectrum obtained after 51 days (Figure 6a) showed little overall conversion of HD to products, and no unusual features were present in the <sup>27</sup>Al MAS NMR spectrum (Figure 6b). Thus, no evidence of a surface alkoxide (Scheme 1) was found. Such species yield resonances between 70 and 80 ppm in <sup>13</sup>C MAS NMR spectra.<sup>25</sup> If formed, alkoxides would presumably undergo facile hydrolysis and thus are not stable in the presence of water. Addition of 33 wt % H<sub>2</sub>O to the sample effected hydrolysis of the HD to the H-2TG and CH-TG sulfonium ions within 17 days (Figure 6c). The H-2TG slowly decomposed to yield CH-TG as the exclusive product after 2.5 months (Figure 6d). This behavior is remarkably similar to that of bulk HD droplets in water.<sup>26</sup> The <sup>27</sup>Al MAS NMR spectrum (Figure 6e) showed an extremely sharp peak at 1.3 ppm that is assigned to free, solvated Al(H<sub>2</sub>O)<sub>6</sub><sup>3+</sup>. This species was not observable by <sup>27</sup>Al CP-MAS NMR, consistent with its substantial motion. Surface Al(H<sub>2</sub>O)<sub>6</sub><sup>3+</sup> also formed on addition of 6 M HCl to AP-Al<sub>2</sub>O<sub>3</sub> itself. Finally, AP-Al<sub>2</sub>O<sub>3</sub> completely dissolved in 6 M HCl to yield free Al(H<sub>2</sub>O)<sub>6</sub><sup>3+</sup> as observed by <sup>27</sup>Al NMR. This is important for the reaction of CW agents as their acidic products will react to the core of alumina particles, consuming them in stoichiometric fashion. Moreover, the ability of acid to generate free Al(H<sub>2</sub>O)<sub>6</sub><sup>3+</sup> is a crucial step in the formation of aluminophosphonates from phosphonic acid products (see below).

(25) Pilkenton, S.; Hwang, S.-J.; Raftery, D. *J. Phys. Chem. B* **1999**, *103*, 11152–11160.

(26) Yang, Y.-C.; Szafraniec, L. L.; Beaudry, W. T.; Ward, J. R. *J. Org. Chem.* **1988**, *53*, 3293–3297.

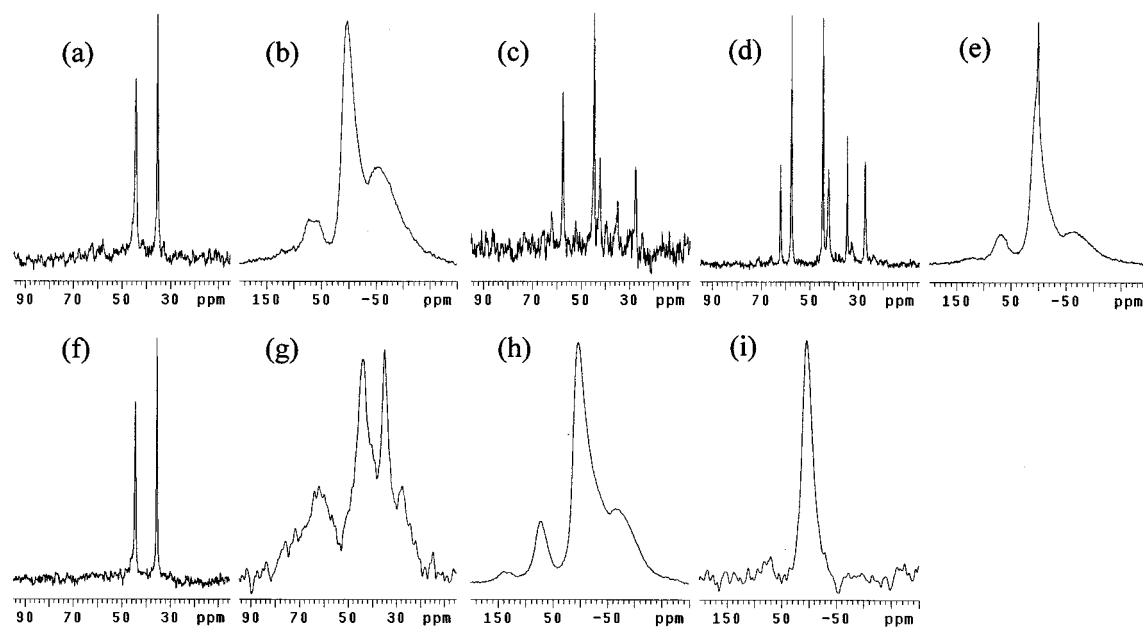


**Figure 6.** MAS NMR spectra obtained for the reaction of 28 wt % HD with "as received" AP-Al<sub>2</sub>O<sub>3</sub>: (a) <sup>13</sup>C, 51 days, (b) <sup>27</sup>Al, 51 days, (c) <sup>13</sup>C obtained 17 days after addition of 33 wt % H<sub>2</sub>O, (d) <sup>13</sup>C obtained 2.5 months after addition of 33 wt % H<sub>2</sub>O, and (e) <sup>27</sup>Al obtained 2.5 months after addition of 33 wt % H<sub>2</sub>O. MAS NMR spectra obtained for the reaction of 28 wt % HD with AP-Al<sub>2</sub>O<sub>3</sub> dried at 100 °C after 4 months: (f) <sup>13</sup>C, (g) <sup>13</sup>C CP, (h) <sup>27</sup>Al, and (i) <sup>27</sup>Al CP.

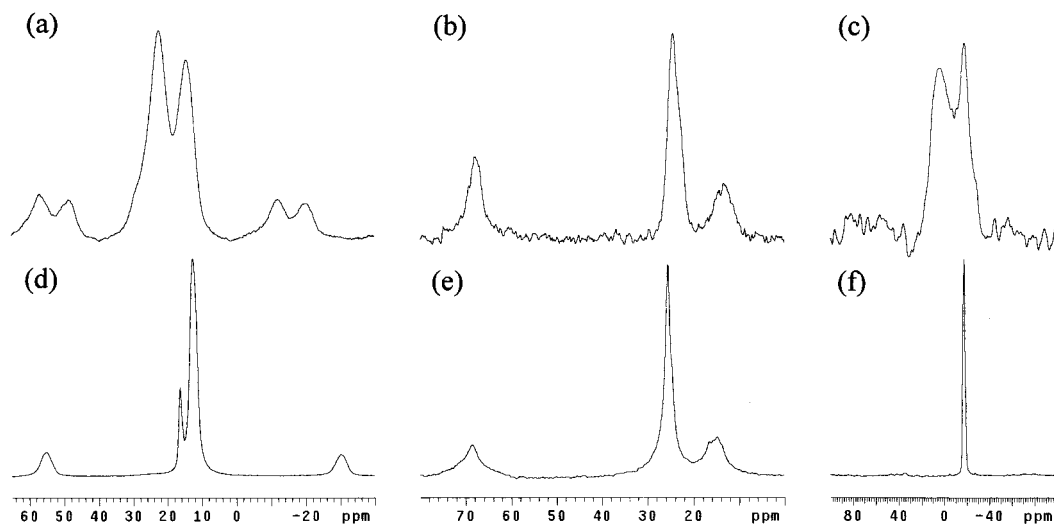


**Figure 7.** MAS NMR spectra obtained after 2 weeks for the reaction of 26 wt % GB with "as received" AP-Al<sub>2</sub>O<sub>3</sub>: (a) <sup>31</sup>P CP, (b) <sup>13</sup>C CP, and (c) <sup>27</sup>Al CP. MAS NMR spectra obtained after 2 weeks for the reaction of 26 wt % GB with model compound **1**: (d) <sup>31</sup>P, (e) <sup>13</sup>C CP, and (f) <sup>27</sup>Al CP.

A second sample was prepared containing 30 wt % HD on AP-Al<sub>2</sub>O<sub>3</sub> dried at 100 °C to remove physisorbed water. <sup>13</sup>C and <sup>27</sup>Al DP and CP-MAS spectra obtained for this sample are also shown in Figure 6. As for the "as received" material, the extent of reaction was not great after an extended period. After 4 months, <sup>13</sup>C MAS revealed mostly unreacted HD (Figure 6f). However, <sup>13</sup>C CP-MAS NMR (Figure 6g) did detect some minor products: a broad peak at 62.1 ppm assignable to TG hydrogen bonded to the surface,<sup>25</sup> and a broad shoulder extending to 80 ppm consistent with the anticipated surface TG alkoxide.<sup>9,25</sup> <sup>27</sup>Al DP and CP-MAS spectra (Figure 6h,i) did not reveal any changes in either the *T<sub>d</sub>* or *O<sub>h</sub>* sites. The non-observance of a <sup>27</sup>Al MAS peak for the surface alkoxide could be attributed to low concentration, overlap of this signal with the surface peak, and/or a large *Q<sub>cc</sub>* for this species. Also, no free Al<sup>3+</sup> was observed in the spectra; excess water is apparently crucial to its formation.

In Figure 7, <sup>31</sup>P, <sup>13</sup>C, and <sup>27</sup>Al CP-MAS spectra obtained after 2 weeks for 26 wt % GB reacted with "as received" AP-Al<sub>2</sub>O<sub>3</sub> are shown along with <sup>31</sup>P MAS and <sup>13</sup>C and <sup>27</sup>Al CP-MAS NMR spectra of **1**. In the <sup>31</sup>P CP-MAS NMR spectra of GB/AP-Al<sub>2</sub>O<sub>3</sub>, two broad peaks are observed at 22.5 and 14.4 ppm which possess intense spinning sidebands, indicative of two distinct, immobilized phosphonates. Extraction of the surface species and analysis by <sup>31</sup>P NMR found only isopropyl methylphosphonic acid (IMPA), but no methyl phosphonic acid (MPA), a potential secondary hydrolysis product (Scheme 1). Thus the two resonances detected in the <sup>31</sup>P CP-MAS spectrum reflect IMPA in two different environments. The <sup>13</sup>C CP-MAS spectrum does not differentiate the two IMPA's, detecting only single P-OiPr and P-CH<sub>3</sub> groups. The <sup>27</sup>Al CP-MAS NMR spectrum reveals a new, sharp peak at -17.9 ppm not present in the pristine AP-Al<sub>2</sub>O<sub>3</sub>. Comparison of these spectra with those of model compound **1** reveals that **1** itself is forming on the AP-Al<sub>2</sub>O<sub>3</sub>

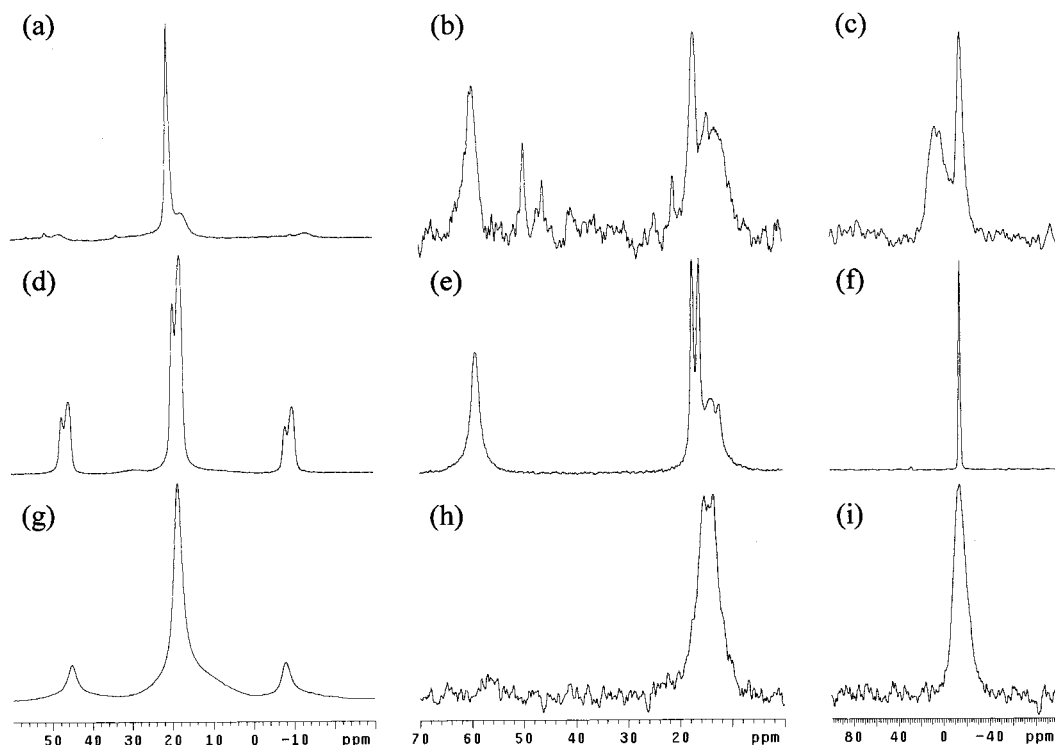


**Figure 8.** MAS NMR spectra obtained after 7 weeks for the reaction of 40 wt % VX with "as received" AP-Al<sub>2</sub>O<sub>3</sub>: (a) <sup>31</sup>P, (b) <sup>13</sup>C CP, and (c) <sup>27</sup>Al CP. MAS NMR spectra obtained for model compound **3**: (d) <sup>31</sup>P, (e) <sup>13</sup>C CP, and (f) <sup>27</sup>Al CP. MAS NMR spectra obtained for model compound **4**: (g) <sup>31</sup>P, (h) <sup>13</sup>C CP, and (i) <sup>27</sup>Al CP.

surface as the <sup>31</sup>P MAS and <sup>27</sup>Al CP-MAS NMR peaks of **1**, 12.6 and -17.6 ppm, respectively, are in close agreement with the peaks detected for one of the surface species (14.4 and -17.9 ppm). The surface complex giving rise to the <sup>31</sup>P CP-MAS NMR peak at 22.5 ppm is consistent with the type of surface complex shown in Scheme 1, and its shift is in agreement with those of the EMPA and PMPA surface complexes observed for the low-loading VX and GD samples (23.0 and 24.0 ppm, respectively). No distinct <sup>27</sup>Al CP-MAS NMR peak is detected for this surface complex, and this is attributed to the potentially large *Q<sub>cc</sub>* for this species and/or its overlapping with the alumina surface *O<sub>h</sub>* peak. Compound **1** (also **2** and **3**, see below) must possess a small *Q<sub>cc</sub>* as evidenced by the sharp <sup>27</sup>Al MAS NMR line width, implying nearly ideal *O<sub>h</sub>* symmetry. The idealized structure is shown in Figure 1.

<sup>31</sup>P MAS and <sup>13</sup>C and <sup>27</sup>Al CP-MAS spectra were obtained for 32 wt % GD reacted with "as received" AP-Al<sub>2</sub>O<sub>3</sub> after 2 weeks, and compared to <sup>31</sup>P and <sup>27</sup>Al MAS and <sup>13</sup>C CP-MAS NMR spectra of model compound **2**. Like GB, two broad peaks possessing intense spinning sidebands are observed for two phosphonate species in the <sup>31</sup>P MAS NMR spectrum at 23.4 and 14.3 ppm, and a new peak is observed in the <sup>27</sup>Al CP-MAS NMR spectrum at -12.2 ppm. Extraction of the surface species and analysis by <sup>31</sup>P NMR found only pinacolyl methylphosphonic acid (PMPA), but no MPA. Thus the resonances found for the two surface phosphonates are similarly assigned to surface-bound PMPA and the discreet aluminophosphonate complex **2**. The shifts of the GD-derived aluminophosphonate species are consistent with those of **2** (<sup>31</sup>P 14.3 ppm; <sup>27</sup>Al -16.7 ppm), and the <sup>31</sup>P MAS NMR shift of the surface-bound PMPA is in agreement with the same species observed in the low-loading sample (24 ppm). As seen for GB, the <sup>13</sup>C CP-MAS NMR spectrum does not distinguish the two PMPA species, yielding only peaks for single O-pinacolyl and P-CH<sub>3</sub> groups. The surface-bound PMPA complex also does not yield a distinct

<sup>27</sup>Al CP-MAS peak (see above). The conversion of surface-bound phosphonate to its aluminophosphonate complex is not as complete as observed in the GB reaction as evidenced by the relatively diminutive <sup>31</sup>P and <sup>27</sup>Al peaks of the aluminophosphonate complex compared to those of the surface-bound IMPA and alumina surface *O<sub>h</sub>* peaks, respectively.

In Figure 8, <sup>31</sup>P MAS and <sup>13</sup>C and <sup>27</sup>Al CP-MAS spectra obtained after 7 weeks for 40 wt % VX reacted with "as received" AP-Al<sub>2</sub>O<sub>3</sub> are shown along with <sup>31</sup>P MAS and <sup>13</sup>C and <sup>27</sup>Al CP-MAS NMR spectra of model compounds **3** and **4**. For VX, the <sup>31</sup>P MAS NMR spectrum is quite different from those of GB and GD in that the main peak at 21.0 ppm is sharp with diminutive spinning sidebands, indicating a rather mobile species. The second <sup>31</sup>P MAS NMR peak at 17.3 ppm is broad and possesses the spinning sidebands expected for a rigid species. Further note the absence of any detectable resonance (ca. 40 ppm) for toxic EA-2192. Extraction and analysis by <sup>31</sup>P NMR also did not detect any EA-2192, but did find both EMPA (32.2 ppm) and MPA (22.6 ppm) in the same proportion as the two phosphonate species evident in the <sup>31</sup>P MAS spectrum. Thus unlike the GB and GD reactions, secondary hydrolysis has occurred to yield MPA. The shift of the sharp <sup>31</sup>P MAS NMR peak at 21.0 ppm is in closest agreement with the 19.7 ppm peak of model compound **3**; thus this peak is assigned to **3** which is quite mobile on the surface and presumably heavily hydrated (to be discussed further below). Consistent with the evident mobility of hydrated, surface **3**, wet, "gummy" samples of authentic **3** also yielded <sup>31</sup>P MAS NMR spectra possessing small spinning sidebands. The MPA species yielding the broad peak at 17.3 ppm is consistent with either a surface-bound MPA species (Scheme 1) or aluminophosphonate complex **4**. The <sup>13</sup>C CP-MAS NMR spectra of the VX-derived species reveal resonances for the O-Et and PCH<sub>3</sub> groups of the EMPA species; the latter overlapping with the PCH<sub>3</sub> of the MPA. Other small, sharp resonances are due to the cleaved thiol (Scheme 1). The



$^{13}\text{C}$  CP-MAS spectrum of **3** reveals, in addition to the expected doublet of the  $\text{PCH}_3$  group ( $J_{\text{PC}}$  ca. 130 Hz), splittings in the  $\text{O-CH}_2\text{CH}_3$  and  $\text{PCH}_3$  sites, but not the  $\text{O-CH}_2\text{CH}_3$  site. These additional “doublets”, which are not observed for VX-derived **3**, may reflect the two different crystal modifications suggested by the  $^{31}\text{P}$  spectra or, perhaps more likely, the presence of two inequivalent sites in the unit cell as they appear to be of equal intensity. These different sites may not be observed in VX-derived **3** due to the extreme hydration and the resulting motion/site averaging. Indeed, such site splittings are not observable in “wet” samples of authentic **3**. The  $^{13}\text{C}$  CP-MAS spectrum of **4** exhibits the expected doublet ( $J_{\text{PC}}$  ca. 133 Hz) for the  $\text{PCH}_3$ , with no additional splittings.

For the VX reaction the conversion of surface-bound phosphonate to its aluminophosphonate complex is essentially complete as evidenced by the  $^{31}\text{P}$  MAS NMR spectra. This is also indicated by the rather intense  $^{27}\text{Al}$  CP-MAS NMR peak detected for this species relative to the  $\text{AP-Al}_2\text{O}_3$  surface  $O_h$  peak. The  $^{27}\text{Al}$  CP-MAS peak evident for the heavily hydrated VX-derived **3** at  $-15.5$  ppm is quite sharp, and consistent with the sharp  $-14.9$  ppm peak observed for model compound **3**. Although the  $^{27}\text{Al}$  MAS NMR shift of the VX-derived species is also consistent with that of model compound **4** ( $-14.6$  ppm), the line width of this resonance is quite broad and inconsistent with the sharpness of the peak for aluminophosphonate species **3**. The broadness of the  $^{27}\text{Al}$  MAS NMR peak for the MPA aluminophosphonate model compound suggests a larger  $Q_{\text{cc}}$  for these aluminum sites, perhaps due to distortions of ideal  $O_h$  symmetry induced by MPA bridging of the sites necessary to maintain charge balance. One possible disruption of the  $O_h$  symmetry is shown in the hypothetical structure in Figure 1 where two bidentate phosphonates bind in equatorial fashion (net charge  $-1$ ) and two monodentate phosphonates bind in the axial positions (net charge  $-2$ ). Consequences to the electric field gradient experienced by the aluminum center are quite obvious in this structure, thus the larger apparent  $Q_{\text{cc}}$  of **4** relative to compounds **1–3**.

**Nature and Importance of the Agent-Derived Aluminophosphonates.** The GB-derived and GD-derived complexes, **1** and **2**, respectively, are insoluble in neutral water and are not hygroscopic. Indeed, they spontaneously precipitate on mixing  $\text{Al}(\text{NO}_3)_3$  with IMPA and PMPA in water. Compound **4**, which precipitates near pH 3, is also insoluble in neutral water and is not hygroscopic. However, the VX-derived complex, **3**, does not precipitate on mixing the precursors, is extremely hygroscopic, and can only be isolated by drying. Anhydrous and hydrated crystalline phases are known for other metal phosphonate complexes.<sup>27</sup> The fact that **3** yields two  $^{31}\text{P}$  MAS NMR peaks with intense spinning sidebands strongly suggests the presence of two rigid, crystalline phases. The two phases detected for **3** may indeed be the anhydrous and hydrated phases. Only one crystalline phase is evident for compounds **1**, **2**, and **4**.

In the environment, nerve agents in contact with aluminum metal could produce aluminophosphonates as the phosphonic acid hydrolysis products would effect corrosion. Such reactions with aluminum and other metals of interest are currently being investigated. If the aluminophosphonate compounds formed

possess adequate stability to be persistent in the environment, they may provide forensic evidence for the former presence of nerve agents. The stability of IMPA and PMPA toward secondary hydrolysis to MPA, combined with their spontaneous reaction in the presence of aluminum ion to form their aluminophosphonate complexes, and the insolubility of these complexes except at low pH strongly suggest that compounds **1** and **2** are viable environmental markers for GB and GD, respectively. As for VX, although EMPA forms compound **3** in the presence of aluminum ion, the complex is soluble at neutral pH and would be quickly dispersed and diluted in a wet environment. However, EMPA is also prone to secondary hydrolysis to yield MPA. This would allow the spontaneous formation of compound **4** at  $\text{pH} \geq 3$ , and this compound is insoluble at neutral pH. Thus compound **4** is the viable environmental marker for VX, whereas GB and GD would not be anticipated to form this compound.

**Outlook for CWA Decontamination.** The room-temperature reactivity exhibited by  $\text{AP-Al}_2\text{O}_3$  for VX, GB, GD, and HD is promising for the use of such a material for “hasty” battlefield decontamination, where CWA deposited on personnel, equipment, vehicles, and perhaps even strategic locations could be quickly removed, adsorbed, and subsequently detoxified. Such reactive materials would also be useful in building, vehicle, and aircraft filtration systems designed to protect occupants against CWA attacks, perhaps extending the life of conventional carbon-based (nonreactive) filters. Finally, the fact that this material can consume large quantities of CWA (essentially a stoichiometric reaction for the nerve agents) is promising for its use in the large-scale decontamination/demilitarization of CWA stockpiles and/or munitions.

## Conclusions

$\text{AP-Al}_2\text{O}_3$  undergoes room-temperature reactions with VX, GB, GD, and HD. The reactive capacity is exceedingly large for the nerve agents as their surface-bound phosphonic acid hydrolysis products effect facile erosion of the alumina surface to form bulk aluminophosphonate complexes. Thus their reactions proceed to the particle core. Aluminophosphonates **1**, **2**, and **4** have been identified as potential forensic markers for GB, GD, and VX, respectively, owing to their insolubility at neutral pH. The reactive capacity for HD is more limited, with higher loadings requiring copious amounts of water to effect facile hydrolysis. TG is the preferred product at low loadings, but sulfonium ions H2-TG and CH-TG exclusively form under high loading/wet conditions. This behavior is analogous to the hydrolysis of bulk HD droplets in water. On  $\text{AP-Al}_2\text{O}_3$  dried to remove physisorbed water, HD yields a species consistent with the alkoxide of TG.

**Supporting Information Available:** Plots of  $^{27}\text{Al}$  MAS NMR intensity gain vs percent weight gain for the series of spectra shown in Figure 2; variable-temperature  $^{27}\text{Al}$  MAS NMR spectra obtained for PD  $\gamma$ -alumina; and  $^{31}\text{P}$ ,  $^{13}\text{C}$ , and  $^{27}\text{Al}$  MAS NMR spectra obtained for the reaction of 32 wt % GD with “as received”  $\text{AP-Al}_2\text{O}_3$  and compound **2** (PDF). This material is available free of charge via the Internet at <http://pubs.acs.org>.

JA003518B

(27) Cunningham, D.; Hennelly, P. J. D. *Inorg. Chim. Acta* **1979**, *37*, 95–102.